ELSEVIER

Nuclear Instruments and Methods in Physics Research B 161–163 (2000) 65–75

NIM B
Beam Interactions with Materials & Atoms

www.elsevier.nl/locate/nimb

# Electronic sputtering of solids by slow, highly charged ions: Fundamentals and applications

T. Schenkel [a,*], M.W. Newman [a], T.R. Niedermayr [a], G.A. Machicoane [a], J.W. McDonald [a], A.V. Barnes [a], A.V. Hamza [a], J.C. Banks [b], B.L. Doyle [b], K.J. Wu [c]

[a] *Lawrence Livermore National Laboratory, University of California, P.O. Box 808, L-414 Livermore, CA 94550, USA*
[b] *Sandia National Laboratory, Albuquerque, NM, USA*
[c] *Charles Evans and Associates, Redwood City, CA, USA*

**Abstract**

Electronic sputtering in the interaction of slow ($v < v_{Bohr}$), highly charged ions (SHCI) with solid surfaces has been subject of controversial discussions for almost 20 years. We review results from recent studies of total sputtering yields and discuss distinct microscopic mechanisms (such as defect mediated desorption, Coulomb explosions and effects of intense electronic excitation) in the response of insulators and semiconductors to the impact of SHCI. We then describe an application of ions like $Xe^{44+}$ and $Au^{69+}$ as projectiles in time-of-flight secondary ion mass spectrometry for surface characterization of semiconductors. © 2000 Elsevier Science B.V. All rights reserved.

*PACS:* 79.20.Rf; 34.50.Fa; 82.80.Ms
*Keywords:* Electronic sputtering; Highly charged ions; Surface analysis; Coincidences

## 1. Introduction

Continuous development of ion source technology in recent years has made beams of slow ($v < v_{Bohr} = 2.19 \times 10^6$ m/s), highly charged ions (SHCI) available for ion–solid interaction studies [1–3]. It is the defining characteristic of SHCI that their charge state, $q$, is much larger than the mean equilibrium charge state which ions develop when traveling in solids with comparable velocities. The latter are about 1+ for $v \ll v_{Bohr}$. Consequently, SHCI neutralize and de-excite rapidly when they interact with a solid surface. Mean charge equilibration times of SHCI like $Xe^{44+}$ and $Th^{75+}$ in thin carbon foils have been found to be only 7 fs [4]. The loss of kinetic energy of ions to target electrons and nuclei is significantly enhanced during charge equilibration [5–8]. The potential energy of SHCI, i.e., the sum of the binding energies of the electrons removed from the ion, is dissipated during de-excitation. This potential energy, 51 and 198 keV for $Xe^{44+}$ and $Th^{75+}$, respectively, is deposited initially in a nanometer size target volume close to the surface. The equivalent power density in this process is $\sim 10^{14}$ W/cm$^2$. De-excitation

* Corresponding author. Fax: +1-925-422-5940.
*E-mail address:* schenkel@llnl.gov (T. Schenkel).

0168-583X/00/$ - see front matter © 2000 Elsevier Science B.V. All rights reserved.
PII: S0168-583X(99)00880-0

begins above surfaces by the resonant capture of target electrons and the formation of a hollow atom. Except for grazing incident collisions, only a small fraction of the potential energy can be dissipated before ions reach the surface, because the available time is too short for relaxation through Auger and radiative transitions. Hollow atom formation and decay in and above metallic and insulating targets has been investigated in great detail by measurements of secondary electron emission, Auger electron and X-ray spectroscopy [1–3]. Atomic force microscopy has been applied to the characterization of nanometer size defects on mica [2,9], highly oriented pyrolitic graphite [10] and alkyl self-assembled monolayers on Si(1 1 1) [11] formed by the impact of individual SHCI. SHCI have also been found to efficiently develop resist materials such as poly(methymethacrylate) and alkanethiolate self-assembled monolayers on gold substrates and masked ion beam lithography has been demonstrated for $Xe^{44+}$ [12,13].

Insulators, semiconductors and thin semimetals react to the intense, ultrafast electronic excitation imposed by SHCI with the emission of large numbers of secondary ions and neutrals. A theory of electronic sputtering by SHCI has to describe microscopic mechanisms for the transfer of projectile potential energy, or electronic excitation energy, into kinetic energy of sputtered particles. Defect mediated sputtering by SHCI up to $Xe^{27+}$ has been demonstrated for CsI, LiF and $SiO_2$ [14–18]. Sputtering by Coulomb explosions [14,19,20] was found to be consistent with results for uranium oxide and SHCI like $Xe^{44+}$ and $Th^{70+}$ [21]. A third model considers effects of high densities of electronic excitation on the structural stability of solids. This approach can explain the very large sputter yields found for GaAs under impact of $Th^{70+}$ [22]. In the following, we will discuss experimental challenges in measurements of sputtering yields (Section 2) before reviewing results from sputter yield measurements in the light of complementary theories (Section 3).

The finding of secondary ion intensities in the order of 0.1–5 secondary ions detected per SHCI [23–25] stimulated interest in the development of SHCI-based surface analysis in a time-of-flight secondary ion mass spectrometry scheme [23–28]. Secondary ion production was found to be dominated by the projectile charge and largely independent of projectile velocity [21,23–25]. The detection of more than one secondary ion from one impact event with high enough probability (>0.01) allows for the analysis of correlations in secondary ion emission. Since multiple secondary ions are emitted by individual projectiles from an area of only a few tens of $nm^2$, coincidence analysis can deliver information on chemical structure and composition of materials on a nanometer length scale [27]. We will present results on the characterization of sub-micron copper lines and copper particles on $SiO_2$ by this approach in Section 4.

## 2. Experimental techniques for sputter yield measurements

Two established techniques for the measurement of sputter yields in particle solid interactions are the micro-balance and the catcher techniques. The former uses a quartz crystal to monitor the change in resonance frequency associated with the mass change of the irradiated surface as a function of exposure time. Thin films of the materials of interest are deposited onto the front electrode which covers the oscillator quartz crystal [3,17]. The sensitivity of this technique has been extended to allow for measurements of mass changes as low as $10^{-3}$ monolayers [3]. While this sensitivity is impressive, application of the micro-balance technique for measurement of sputter yields in the order of 10 atoms removed per projectile requires a beam current of a few nA or about $10^{10}$ projectiles per second. Beam currents of this order are routinely extracted from ECR sources but only for ions with charge states below about 30+ for xenon.

In the catcher or collector technique, sputtered particles are collected on a secondary target for in situ or ex situ analysis after accumulation of a sufficiently high surface coverage [14,29]. Recently, Mieske et al. [30] have reported on in situ analysis of catcher targets in studies of sputtering yields of metals by high energy heavy ions ($\sim$1 MeV/u).

Using a 1.5 MeV carbon beam they were able to detect Ti on Si at coverages in the low $10^{13}$ atoms/cm$^2$ range. This sensitivity is comparable to the sensitivity of the micro-balance technique. An advantage of the catcher technique lies in the fact that sputter targets can be bulk single crystals as compared to the restriction to thin films that is given in measurements with the micro-balance technique [3].

For the sputter yield measurements with SHCI from the EBIT (electron beam ion trap) at Lawrence Livermore National Laboratory [1,2], collectors consisted of thin (50–150 nm) $SiO_2$ layers on silicon substrates. In order to maximize the collection efficiency, catcher targets were placed at a distance of 6 mm from the sputter targets, resulting in a view factor of 0.1. Beams of SHCI at 0.3 $v_{Bohr}$ impinged on GaAs and $UO_2$ targets with an incident angle of 30°. Targets were cleaned in situ by low energy ion sputtering ($UO_2$) or cycles of low energy ion sputtering and annealing to 600° K (GaAs). Surface conditions were monitored by secondary ion mass spectrometry with highly charged projectiles (HCI–SIMS) [1,21,22]. Beam intensities for extraction of SHCI from an EBIT are in the order of $10^6$ $Xe^{44+}$/s and $10^5$ $Au^{69+}$/s. At a sputtering yield of 10 atoms per projectile, surface coverages of sputtered materials after exposure times of several days are only in the order of $10^{11}$ atoms/cm$^2$. Quantitative analysis of catcher targets was performed at the heavy ion backscatter facility at Sandia National Laboratory [31–33] using beams of 100 KeV carbon ions. The sensitivity of HIBS for detection of heavy elements on otherwise clean silicon is in the order of $10^9$ atoms/cm$^2$. In Fig. 1 we show an example of HIBS analysis of a catcher target (150 nm $SiO_2$ on Si) with a uranium coverage of 3.3 $(\pm 0.3) \times 10^{11}$ atoms/cm$^2$.

Relative uncertainties in sputter yields determined with the collector technique result from uncertainties in HIBS results, dose uncertainties, and variations in the view factors between measurements and range typically from ±10% to 30%. One contribution to the systematic error stems from assumptions on sticking probabilities of secondary particles on the catcher surface. Typical values for the latter are >0.9 [34]. Another uncertainty lies in the assumption of a cosine angular distribution of secondary particles in the calculation of the view factor. Analysis of catcher targets is a standard technique for the determination of actual angular distributions of secondary neutrals [29]. This approach requires a distance between target and collector that is large compared to the spot size of the primary beam. The increased target–collector distance corresponds to a reduction in the achievable surface coverage. With the current beam intensity limitations for SHCI such a reduction of surface coverage was prohibitive in our experiments. Overall systematic uncertainties for sputtering yield values determined for SHCI from EBIT with the catcher technique are about ±50%.

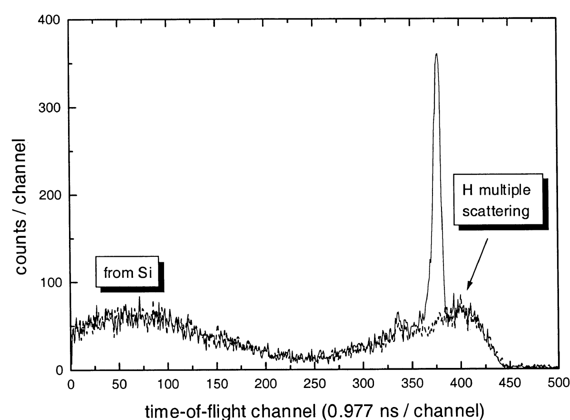


Fig. 1. Heavy ion backscattering spectrum from of a U–$SiO_2$ (150 nm on Si) catcher target (solid) and an unexposed witness target (dashed). Projectiles were carbon at 100 keV. The incident charge was 10 μC. The uranium coverage was 3.3 $(\pm 0.3) \times 10^{11}$ atoms/cm$^2$.

Secondary ion yields from GaAs and $UO_2$ samples were measured by time-of-flight secondary ion mass spectrometry with SHCI as projectiles [23–28]. Briefly, SHCI are extracted from EBIT and impinge on samples under normal incidence for analysis in a low resolution, high transmission instrument. Samples are biased to a few thousand volts positive or negative bias and secondary ions are accelerated to an extraction grid and then drift to an annular microchannel plate detector. The detection efficiency of this arrangement is 0.1–0.15. Time-of-flight cycles are started by secondary

electrons or protons that are emitted following the impact of individual projectiles. This single ion triggering scheme allows for a timing resolutions of 1 ns and a start efficiency of practically 100% in negative polarity and >80% in positive polarity for SHCI like $Xe^{44+}$. Conventional TOF–SIMS instruments use electronic starts derived from bunched ion pulses and can achieve the nanosecond timing resolution needed for competitive mass resolution [35]. This approach is impractical for SHCI at the currently available beam intensities. For catcher analysis, secondary ions were extracted into a reflectron type time-of-flight spectrometer with a mass resolution, $m/\Delta m$, of 1000 at $m = 28$ u [28].

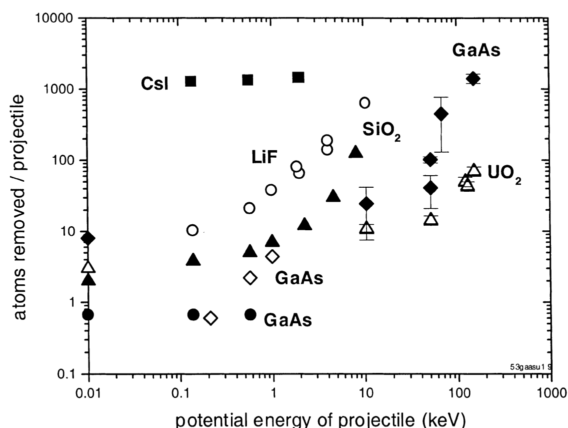


Fig. 2. Total sputtering yields for CsI, solid squares [14]; LiF, open circles [15–18]; $SiO_2$, solid triangles [17,18]; GaAs, solid circles [17,18], open diamonds [36,37], solid diamonds [22]; and $UO_2$ [21] versus potential energy of projectile. Kinetic energies of projectiles were constant within each data set but varied in measurements by different groups.

## 3. Sputter yields of solids under impact of slow, highly charged ions

Results from sputter yield measurements for CsI [14], LiF [15–18], $SiO_2$ [17,18], GaAs [17,18,22,36,37] and $UO_2$ [21] are shown in Fig. 2 as a function of potential energy of SHCI [1].

### *3.1. Defect mediated sputtering*

Desorption yields of several hundred atoms per projectile for LiF and $SiO_2$ were determined by the micro-balance technique and with decelerated (~1 keV) beams of SHCI up to $Xe^{27+}$. These results have been interpreted with a model of defect-mediated desorption [3,14,17,18,38,39]. Here, electronic sputtering results from the formation and successive decay of electronic defects such as self-trapped excitons and self-trapped holes. Microscopic mechanisms of defect formation which have been established for photon and electron irradiation of materials were applied also to the response of solids to the impact of SHCI. In ESD (electron stimulated desorption), energetic electrons transfer kinetic energy to target electrons through inelastic collisions [40]. In materials such as alkali halides and $SiO_2$, the excitation of electrons from the valance band leads to a strong local deformation of the crystal lattice field. It is energetically favorable for the excited hole or electron to be immobilized by this distorted field. Both electrons or holes can be self-trapped and one speaks of "self-trapped exitons" [41]. In the example of alkali halides such as LiF, excitation of electrons in the valance band opens the possibility of covalent bonding of fluorine atoms in the form of halide dimers, $F_2^-$ [41]. Formation of stable chemical bonds in the excited state is essential for the trapping of the electronic excitation. Following the excitation of the valence electron, free holes have a finite range before self-trapping. Average self-trapping times of holes in alkali halides have been estimated to be about 100 fs [40,41]. In materials without this strong electron–lattice coupling, such as metals and semiconductors, excited electrons thermalize in collisions with lattice atoms or recombine with holes in the valance band and the electronic excitation is not stabilized in a permanent lattice distortion. Self-trapped excitons decay into H centers (for LiF : $F_2^-$ at an anion site) and F centers (for LiF: $e^-$ at an anion site). At target temperatures of a few hundred degrees Celsius, thermal hoping motion of these color centers can be activated and a fraction of the defects can diffuse to the target surface. When reaching the surface, the $F_2^-$ configuration becomes energetically unfavorable and the H center decays into $F^-$ and $F^0$ were the neutral fluorine atom is weakly bound and readily

desorbs. F centers can neutralize a $Li^+$ ion at the surface. Weakly bound $Li^0$ can then be desorbed thermally or through momentum transfer from incident projectiles that impinge on the sample in close vicinity. In ESD from ideal crystals at elevated temperatures and at low excitation densities ($\ll 10^{18}$ $e^-$–hole pairs/cm$^3$), the number of molecules removed from the surface can be expected to be close to the number of electron–hole pairs generated in the crystal by an energetic electron [40].

The reason for the applicability of an ESD model to SHCI stimulated desorption lies in the fact that SHCI reach charge state equilibrium in solids mostly through Auger transitions [1,3,4] rather than the emission of energetic photons. Inelastic mean free paths of e.g. 500 eV electrons in silicon are only a few nm [42]. Consequently, energetic electrons undergo many inelastic collisions in a process referred to as cascade multiplication [40,43]. After a few tens of fs, the energy of the ionizing radiation is transferred to a number of low energy holes and electrons with energies below the minimum energy required for ionization. SHCI, as well as other forms of ionizing radiation such as singly charged ions, fast heavy ions [49] and energetic electrons [40] deposit a fraction of their initial energy in the formation of electron–hole pairs. Important differences with respect to the response of solids to different forms of electronic excitation lie in the density of the electron–hole plasma, and the degree of lattice heating accompanied by the electronic excitation.

In their study of CsI under impact of 60 keV $Ar^{q+}$ ($q = 4$ to 11+), Weathers et al. [14] have measured desorption yields of about 1300 atoms/ion. The contribution from collisional sputtering due to transfer of kinetic energy of projectiles to target atoms in elastic collisions is only in the order of 1–10 atoms/ion. The effect of potential energy deposition when increasing the charge state from $q = 4+$ ($E_{pot} = 0.138$ keV) to $q = 11+$ ($E_{pot} = 2.01$ keV) was significant but the total desorption yield was dominated by transfer of kinetic energy of projectiles to target electrons through electronic energy loss processes. Self-trapped excitons can be formed in CsI and the large desorption yield is consistent with a mechanism of defect mediated sputtering. Sputter yields from $LiNbO_3$ for the same projectiles amounted to only about 0.5 atoms/ion and were consistent with collisional sputtering [14].

### 3.2. Coulomb explosions

An alternative model of electronic sputtering by SHCI is the Coulomb explosion model [19,20,45]. Here, it is assumed that a charged domain is formed at the surface of insulating targets following emission of several hundred electrons in the course of SHCI relaxation. Coulomb repulsion between adjacent, positively charged ions then results in the emission of charged and neutral particles. Surface Coulomb explosions are equivalent to ion explosion spikes which have long been proposed as a mechanism of track formation in dielectric materials following impact of fast heavy ions [46]. Also equivalent is the basic criticism, namely the question whether or not hole lifetimes and hole mobilities allow for a localization of the initial electronic excitation for a time long enough to transfer sufficient momentum so that sputtering is possible. In defect mediated desorption, this localization is achieved by formation of new (meta-)stable bonds. However, electronic excitation of repulsive states does not necessary lead to desorption. This was demonstrated in classical trajectory studies of $F^+$ formation in NaF. Here, it was found that a transition from a repulsive to an attractive lattice configuration followed $F^+$ formation within only 30 fs [47], and this fast lattice rearrangement prevented desorption of the $F^+$. It would be highly desirable to perform such calculations under conditions were excitation densities approach the molecular density. If the formation of stable defects is energetically unfavorable, like in MgO or GaAs, holes will diffuse away from the site of ion impact or they will recombine with target electrons [38,39]. In fact, the absence of sputter yield increases for MgO and GaAs targets as a function of charge for $Ar^{q+}$ ($q < 10+$) was interpreted as evidence against the possibility of sputtering through surface Coulomb explosions [17,18,38,39] and for defect mediated sputtering as the dominant source of surface erosion by SHCI. Sputtering by SHCI is a consequence of electronic

excitation of surfaces much like nuclear tracks are a consequence of the electronic excitation of materials along the path of a swift heavy ion [44,46]. In both cases, lattice rearrangements, damage or ablation result from transfer of kinetic energy from fast projectiles or potential energy from slow, highly charged projectiles to target electrons. The observation of thresholds in the electronic stopping power for the onset of track formation has been important in studies of track formation mechanisms. For materials in which self-trapped excitons can be formed, like LiF and $SiO_2$, these thresholds are a factor 5–10 smaller than for materials where STE cannot be formed (like MgO and GaAs) [44]. Considering this fact, it is plausible that the available potential energy of $Ar^{9+}$ (about 1 keV) is below the threshold for the onset of electronic sputtering in some materials.

The study of uranium oxide with ions up to $Th^{70+}$ has shown evidence for Coulomb explosions [21]. Both total ablation rates and secondary ion yields were found to increase as a function of projectile charge (or potential energy). Also, ionization probabilities, i.e., the number of secondary ions emitted per amount of sputtered material, were found to increase as a function of projectile charge by about an order of magnitude to a value of 5–7%. The detection of high yields of heavy cluster ions such as $(UO_2)_7^+$ and the very pronounced charge state dependency of cluster ion emission point towards contributions from shock waves initiated by surface Coulomb explosions [1,21]. While the energy distribution of atomic, positive ions showed a broadening towards higher initial energies, the overall energies were much smaller than the 100 eV predicted by molecular dynamics simulations of Coulomb exploding silicon surfaces [1,21,48,49]. Surface Coulomb explosions have been proposed as a mechanism for sputtering of protons from hydrocarbon covered surfaces [50]. Aumayr et al. [38,39] argued that this mechanism only applies to light ions which can escape sufficiently fast from the surface to make reneutralization unlikely. We like to point out that Coulomb explosion sputtering can result when momentum transfer through Coulomb repulsion during a given time accelerates surface species to energies sufficient to overcome their surface binding energy. Once accelerated, uranium ions will move 15 times slower than protons but the increased possibility of re-neutralization changes only the ionization probability (i.e., number of emitted ions per neutrals) not the sputtering yield (i.e., number of emitted ions and neutrals). Also, ionization probabilities derived from molecular dynamics simulations of surface Coulomb explosions are comparable to the values found in the study of uranium oxide [49].

A necessary condition for surface Coulomb explosions is the formation of a charge domain at the surface in the course of SHCI relaxation [19–21,36,37,48,49]. Evidence for nanoscopic charging of $SiO_2$ during the relaxation of SHCI like $Xe^{44+}$ and $Th^{75+}$ was observed in electron emission studies [23–25,51]. Electron yields from thin $SiO_2$ films (150 nm on Si) were lower than yields from gold targets, contrary to the general observation of higher electron yields from insulators as compared to metals [43,52,53]. The relative low mobility of holes in $SiO_2$ ($\sim 2 \times 10^{-5}$ $cm^2/Vs$ [54]) leads to an increase of the effective surface barrier during the emission of electrons in an impact event. This effect was already observed to a lesser degree for 200 keV $Xe^{1+}$ impact where the electron yields were about 7 $e^-$/ion [52] as compared to yields of 50 $e^-$/$Xe^{52+}$ [23–25,51]. While the lifetime of the charge domain is not known, a lower limit can be estimated from the relaxation time of the SHCI, which is only 5–10 fs [4,5]. The charge state dependent increase of secondary ion yields from $SiO_2$ films indicate that Coulomb repulsion of positively charged ions at the surface contributes to the ejection of particles into the vacuum [21,23–25]. Positive, atomic ions are ejected from an area close to the impact site of the SHCI were the ionization density is highest, while positively and negatively charged molecular ions and cluster ions are ejected from a larger area surrounding the impact site. Emission of cluster ions like $(SiO_2)_nO^-$, which have been detected up to $n = 24$ [55], is stimulated by the shock wave or pressure pulse which follows the surface Coulomb explosion. Charge states of ions emitted from areas of relatively low ionization density are dominated by their chemical properties (i.e., electron affinity and ionization potential) [26,51]. This situation is analogous to secondary

ion emission following the impact of fast, heavy ions on insulators [56].

Studies of insulators under ion bombardment generally pose experimental problems due to macroscopic charging of target surfaces. In the studies of LiF, targets were heated to increase the ionic conductivity during ion irradiation. For CsI and $SiO_2$, charging was compensated by simultaneous flooding of the target with low energy electrons [14,17,18]. These measures do impose a systematic limitation to the insights gained in these studies since microscopic charging is at the physical basis of the Coulomb explosion mechanism. It seems obvious that investigations of the influence of charge compensation techniques on the characteristics of sputtering by SHCI are mandatory before contributions from different mechanisms can be quantified or before contributions from Coulomb explosions can be ruled out.

The influence of Coulomb repulsion on the energetics of lattice re-arrangements [47] and the self-trapping of dense clusters of excitons [44] is currently not well understood for the high excitation and ionization densities induced by SHCI.

### 3.3. *Effects of intense, ultrafast electronic excitations*

Sputtering of GaAs was investigated by three groups with three different techniques (micro-balance [17,18], catcher target [22], and quadrupole mass spectrometry [36,37]). Interestingly, results were interpreted also with three different models. The absence of yield increases for very slow $Ar^{q+}$ up to 9+ is consistent with the defect-mediated sputtering model since the required defects cannot be formed in GaAs [17,18,38,39]. On the contrary, Mochiji [36,37] reported increasing ablation rates for $Ar^{q+}$ ($q = 1+$ to 9+), and interpreted this finding in terms of a surface Coulomb explosion model. Results from experiments with highly charged xenon and thorium ions showed sputtering yields as high as $1410 \pm 210$ atoms/$Th^{70+}$ [22]. Measurements of secondary ion yields allowed for a determination of the ionization probabilities of secondary ions, and, contrary to expectations from a Coulomb explosion model, the ionization probability was found to decrease for very high charge states. The high sputtering yields for GaAs can be understood when considering the structural stability of covalent solids under conditions of intense, ultrafast electronic excitation induced by de-exciting SHCI [1,22]. This model was initially developed for the description of femtosecond melting of Si and GaAs where high densities ($>10^{21}$ $cm^{-3}$) of electronic excitations are induced by femtosecond lasers [57]. Later on Stampfli [58] recognized that swift heavy ions pose an alternative way for the creation of dense electron–hole plasmas in solids. Electron emission yields in the interaction of SHCI with solids can be in the hundreds, but only a few percent of the potential energy of SHCI is dissipated in this emission channel [59]. Most of the potential energy is deposited in the bulk of the target [1,60]. It must be viewed as a shortcoming of currently available Coulomb explosion models [45,48,49] that they consider only the effects of ionization, while neglecting the much larger part of the potential energy of SHCI that is deposited through electronic excitations in the target bulk. This model has been applied to calculate the effects of electronic excitations on the structural stability of materials such as Si, GaAs and $SiO_2$ [57,58]. In covalent solids, such as silicon, the valence band is of bonding character and the conduction band has anti-bonding character. Electronic excitations weaken the covalent bonds and cause a repulsive force between the atoms. An instability of the atomic structure thus arises on a femtosecond time scale, before hot electrons have transferred their energy to the lattice. A critical excitation density for the onset of femtosecond melting is in the order of the atomic density. In GaAs the zinc blende structure undergoes a phase transformation when about one electron per GaAs molecule is excited from the valence band into the conduction band. A critical laser fluence necessary to induce such a phase transition is $\sim 0.8$ kJ/$m^2$ [57,61], or $\sim 5$ keV/$nm^2$ where characteristic absorption depth are $\sim 1 \mu m$ [62]. These values can be exceeded by SHCI like $Th^{70+}$ ($E_{pot} = 152.6$ keV). Here, the potential energy is deposited during a relaxation time of $\sim 5$ fs and along a path of $\sim 3$ nm [4,5,22].

At the heart of the problem of electronic sputtering by SHCI lies the time dependent response of

target electrons and lattice atoms to the induced perturbation. The time scale for relaxation of SHCI is about 10 fs, while the time scale for lattice motion is 100 fs to tens of ps. The emission of neutral and charged particles (atoms and molecules) from the surface follows the initial excitation after secondary electrons have transferred most of their energy to the lattice. Both hot carrier transport processes and lattice response mechanisms can be expected to depend strongly on the excitation densities generated by SHCI. For a material like $SiO_2$ all three of the processes discussed above are likely to contribute to sputtering by SHCI.

## 4. Applications of slow, highly charged ions surface analysis

The potential of SHCI like $Xe^{44+}$ for applications in surface analysis lies in the fact that these ions produce up to three orders of magnitude more secondary ions than singly charged projectiles [1,11,21–28,63,64].

In HCI–SIMS, each time-of-flight cycle is started by the impact of an individual projectile. Time-of-flight secondary ion mass spectrometry (TOF–SIMS) spectra can be recorded both in histogram mode or in list mode. In the former, TOF-cycles from consecutive projectiles are simply summed up to form a spectrum. Typically, accumulation of cycles from impact of a few million projectiles yields sufficient statistics and accumulation times are about 10 min. In list mode, time-of-flight cycles (i.e., the start trigger and associated stops from secondary ions) from each projectile are stored separately. Then, conditions on the presence of selected mass peaks are selected when TOF-cycles are summed up. The resulting coincidence spectra show correlations between selected secondary ions or molecular ions that were detected. Each projectile forms secondary ions from a surface area with an estimated size of only a few tens of nanometers [11], and the correlations therefore contain considerable information about the local chemical composition.

The correlation coefficient, $C(\mathrm{A,B})$, gives a measure for the probability to detect a secondary ion B in coincidence with ion A [27,64,65]:

$$C(\mathrm{A,B}) = \frac{P(\mathrm{A,B})}{P(\mathrm{A})P(\mathrm{B})}.$$

Here, $P(\mathrm{A})$ and $P(\mathrm{B})$ are the probabilities for the detection of secondary ions A and B independently in all impact events. $P(\mathrm{A,B})$ is the probability for detection of A and B in the same impact event. For $C(\mathrm{A,B}) > 1$, it is more likely to detect A when B is also present. An example of correlation coefficients is given in Fig. 3(a) for secondary ions from the copper interconnect sample [64,66]. The sample consisted of copper lines with a width of 0.8 μm and spacings of 2.4 μm. The copper lines were formed in an $SiO_2$ layer on a Si substrate through

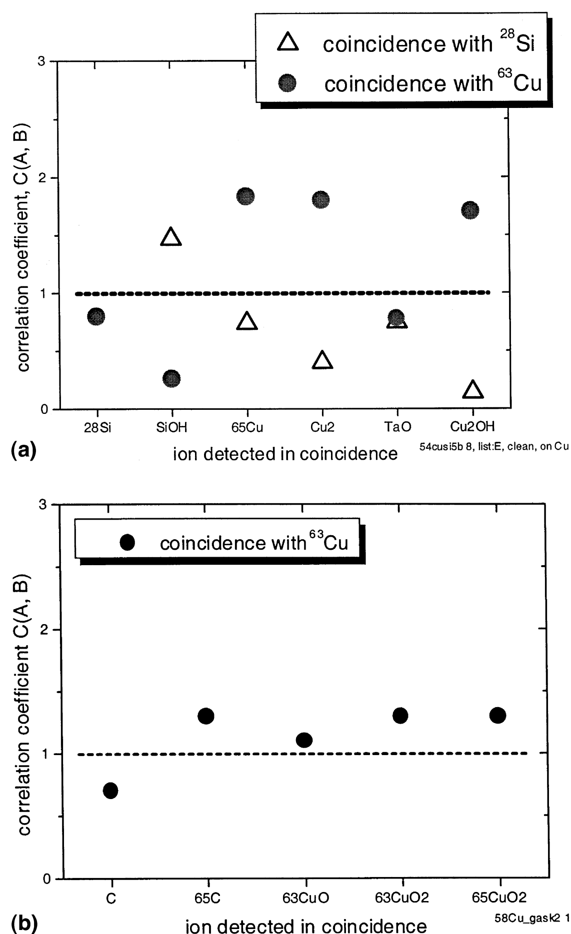


Fig. 3. (a) Correlation coefficients from coincidence analysis of secondary ions from a Cu-interconnect sample [64,66] and (b) from a bulk copper target.

a damascene process [66]. A 25 nm wide Ta layer was used as a diffusion barrier between the copper lines and the oxide. The coincidence analysis shows that the probability to detect a $^{65}Cu^+$ is increased when $^{63}Cu^+$ was also detected in the impact event. $^{65}Cu^+$ and $^{63}Cu^+$ are both emitted when a highly charged ions probes an area on one of the copper lines. On the contrary, $C(A, B) < 1$ indicates an anti-correlation between, e.g., emission of $^{28}Si^+$ and $^{65}Cu^+$ or $^{63}Cu_2^+$. Here, it is very unlikely to detect both a copper and a silicon ion from the same impact event. This anti-correlation is characteristic for well-separated structures of different chemical composition. Statistical uncertainties in values of correlation coefficients are typically smaller than ±20%.

Detection of $TaO^+$ ions from the Ta barrier layer is, at the given level of statistical uncertainly, weakly anti-correlated to both silicon and copper ions. This is expected for a well-separated, intact-barrier layer and also demonstrates that highly charged ions do indeed probe surface features on a length scale of a few tens of nm.

An example of uncorrelated or random emission of secondary ions is shown in Fig. 3(b). Here, the correlation coefficients are close to unity, $C \approx 1$, indicating that copper ions emitted from a bulk copper sample are emitted randomly, without significant correlations.

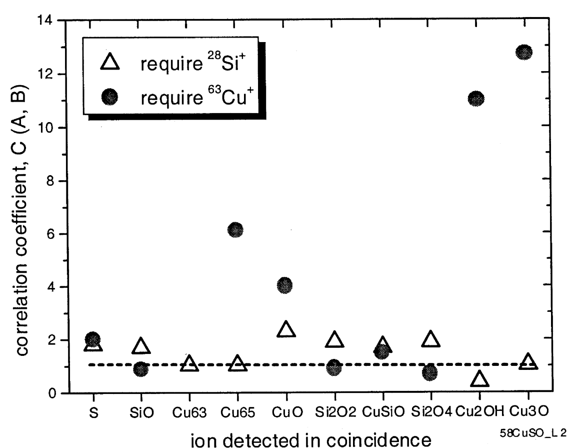


Fig. 4. Correlation coefficients from coincidence analysis of a $CuSO_4/SiO_2$ sample with a copper oxide coverage of about 0.01 monolayers.

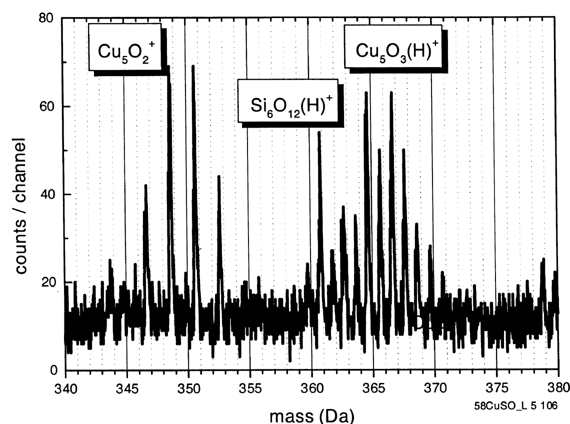


Fig. 5. TOF–SIMS spectrum from the $CuSO_4/SiO_2$ sample with copper oxide and $SiO_2$ cluster ions. Projectiles were $Xe^{48+}$ with a kinetic energy of 557 keV.

In another example of coincidence analysis the sample was a $SiO_2$ wafer which had been coated with $CuSO_4$. The surface coverage of the copper oxide was ~ 0.01 monolayers. Fig. 4 shows correlation coefficients with very strong correlations between copper and copper oxide molecular ions. These correlations indicate the presence of well-separated copper oxide and silicon dioxide areas on the surface and would not be expected for a blanket deposit of evenly separated copper oxide molecules. The latter is energetically unfavorable and the formation of islands has been studied extensively in the context of the early stages of thin film growth. Fig. 5 shows a section of an HCI–SIMS spectrum with positive secondary ions emitted from the $CuSO_4/SiO_2$ sample. The detection of copper oxide clusters is consistent with the presence of copper oxide islands or particles on the surface. Comparison of our results with results from direct imaging techniques [67] is subject of ongoing studies.

## 5. Summary

Data on sputtering yields for the impact of slow, highly charged ions are now available for ions up to $Th^{70+}$ and for insulators (alkali halides, $SiO_2$ and $UO_2$) as well as for one semiconductor

(GaAs). Yields in electronic sputtering by SHCI can exceed yields known from linear collision cascade sputtering by orders of magnitude. Comparing results from materials with distinct electronic properties, it becomes clear that SHCI induced sputtering is a complex phenomena with contributions from several microscopic mechanisms for the transfer of potential energy of projectiles to kinetic energy of sputtered particles. Defect mediated desorption was demonstrated for alkali halides and $SiO_2$ in a regime of relatively low excitation strength (i.e., for charge states <30+ for xenon). Contributions from Coulomb explosions were observed in sputtering and secondary ion production from uranium oxide and for SHCI like $Xe^{44+}$ and $Th^{70+}$. High sputtering yields for GaAs (1400 atom/$Th^{70+}$) can be understood when considering the effects of intense ($10^{14}$ W/cm$^2$), ultrafast (5–10 fs) electronic excitations induced by de-exciting SHCI.

Detection of multiple secondary ions following the impact of individual SHCI allows for the analysis of correlation effects in secondary ion emission. Since each projectile emits secondaries from an area of a few tens of nm$^2$, coincidence analysis can reveal information on chemical structure and composition on a nanometer length scale and with high sensitivity. The presented examples of coincidence analysis of copper structures on silicon dioxide wafers demonstrate the capabilities of this approach. Ongoing studies concern quantitative comparison of HCI–SIMS with established topographical and chemical analysis techniques.

## Acknowledgements

The authors gratefully acknowledge the excellent technical support at the LLNL EBIT facility provided by D. Nelson and E. Magee. This work was performed under the auspices of the US Department of Energy by Lawrence Livermore National Laboratory under contract no. W-7405-ENG-48. Parts of this work were supported by a SBIR grant #50-DKNB-9-90088 from the US Department of Commerce.

## References

[1] T. Schenkel, A.V. Hamza, A.V. Barnes, D.H. Schneider, Prog. Surf. Sci. 61 (1999) 23.
[2] D.H.G. Schneider, M.A. Briere, Phys. Scr. 53 (1996) 228.
[3] A. Arnau, F. Aumayr, P.M. Echenique, M. Grether, W. Heiland, J. Limburg, R. Morgenstern, P. Roncin, S. Schipers, R. Schuch, N. Stolterfoht, P. Varga, T.J.M. Zouros, H. Winter, Surf. Sci. Rep. 27 (1997) 113.
[4] M. Hattass, T. Schenkel, A.V. Hamza, A.V. Barnes, M.W. Newman, J.W. McDonald, T.R. Niedermayr, G.A. Machicoane, D.H. Schneider, Phys. Rev. Lett. 82 (1999) 4795.
[5] T. Schenkel, M.A. Briere, A.V. Barnes, A.V. Hamza, K. Bethge, H. Schmidt-Böcking, D. Schneider, Phys. Rev. Lett. 79 (1997) 2030.
[6] T. Schenkel, A.V. Hamza, A.V. Barnes, D.H. Schneider, Phys. Rev. A 56 (1997) 1701.
[7] M.A. Briere, T. Schenkel, D.H. Schneider, P. Bauer, A. Arnau, Phys. Scr. T 73 (1997) 324.
[8] J.I. Juaristi, A. Arnau, P.M. Echenique, C. Auth, H. Winter, Phys. Rev. Lett. 82 (1999) 1048.
[9] D.C. Parks, M.P. Stockli, E.W. Bell, L.P. Ratkliff, R.W. Schmieder, F.G. Serpa, J.P. Gillaspy, Nucl. Instr. and Meth. B 134 (1998) 46.
[10] K. Mochiji, S. Yamamoto, H. Shimizu, S. Ohtani, T. Seguchi, N. Kobayashi, J. Appl. Phys. 82 (1997) 6037.
[11] T. Schenkel, M. Schneider, M. Hattass, M.W. Newman, A.V. Barnes, A.V. Hamza, R.L. Cicero, C.E.D. Chidsey, D.H. Schneider, J. Vac. Sci. Technol. B 16 (1998) 3298.
[12] L.P. Ratliff, R. Minniti, A. Bard, E.W. Bell, J.D. Gillaspy, D. Parks, A.J. Black, G.M. Whitesides, Appl. Phys. Lett. 75 (1999) 590.
[13] J.D. Gillaspy, D.C. Parks, L.P. Ratkliff, J. Vac. Sci. Technol. B 16 (1998) 3294.
[14] D.L. Weathers, T.A. Tombrello, M.H. Prior, R.G. Stokstad, R.E. Tribble, Nucl. Instr. and Meth. B 42 (1989) 307.
[15] T. Neidhar, F. Pichler, F. Aumayr, H.P. Winter, M. Schmid, P. Varga, Phys. Rev. Lett. 74 (1995) 5280.
[16] T. Neidhar, F. Pichler, F. Aumayr, H.P. Winter, M. Schmid, P. Varga, Nucl. Instr. and Meth. B 98 (1996) 465.
[17] M. Sporn, G. Libiseller, T. Neidhart, M. Schmid, F. Aumayr, H.P. Winter, P. Varga, Phys. Rev. Lett. 79 (1997) 945.
[18] P. Varga, T. Neidhart, M. Sporn, G. Libiseller, M. Schmid, F. Aumayr, H.P. Winter, Phys. Scr. T73 (1997) 307.
[19] I.S. Bitensky, M.N. Murakhmetov, E.S. Parilis, Sov. Phys.-Tech. Phys. 24 (1979) 618.
[20] E.S. Parilis, Z. Phys. D 21 (1991) S127, and references therein.
[21] T. Schenkel, A.V. Barnes, A.V. Hamza, J.C. Banks, B.L. Doyle, D.H. Schneider, Phys. Rev. Lett. 80 (1998) 4325.
[22] T. Schenkel, A.V. Barnes, A.V. Hamza, J.C. Banks, B.L. Doyle, D.H. Schneider, Phys. Rev. Lett. 81 (1998) 2590.
[23] T. Schenkel, A.V. Barnes, M.A. Briere, A.V. Hamza, A. Schach von Wittenau, D.H. Schneider, Nucl. Instr. and Meth. B 125 (1997) 153.

[24] T. Schenkel et al., Mater. Sci. Forum 248–249 (1997) 413.
[25] T. Schenkel et al., Phys. Rev. Lett. 78 (1997) 2481.
[26] T. Schenkel, A.V. Hamza, A.V. Barnes, D.H. Schneider, D.S. Walsh, B.L. Doyle, J. Vac. Sci. Technol. A 16 (1998) 1384.
[27] A.V. Hamza, T. Schenkel, A.V. Barnes, D.H. Schneider, J. Vac. Sci. Technol. A 17 (1999) 303.
[28] T. Schenkel, A.V. Hamza, A.V. Barnes, M.W. Newman, G.A. Machicoane, T.R. Niedermayr, M. Hattass, J.W. McDonald, K.J. Wu, R.W. Odom, D.H. Schneider, Phys. Scr. T80 (1999) 73.
[29] H.H. Andersen, H.L. Bay, in: R. Behrisch (Ed.), Sputtering by Particle Bombardment I, Springer, Berlin.
[30] H.D. Mieske, W. Assmann, M. Brodale, M. Dobler, H. Glückler, P. Hartung, P. Stenzel, Nucl. Instr. and Meth. B 146 (1998) 162.
[31] J.C. Banks, B.L. Doyle, J.A. Knapp, D. Werho, R.B. Gregory, M. Anthony, T.Q. Hurd, A.C. Diebold, Nucl. Instr. and Meth. B 138 (1998) 1223.
[32] J.A Knapp, J.C. Banks, B.L. Doyle, Nucl. Instr. and Meth. B 85 (1994) 20.
[33] B.L. Doyle, J.A. Knapp, D.L. Buller, Nucl. Instr. and Meth. B 42 (1989) 295.
[34] K.G. Liebrecht, J.E. Griffith, R.A. Weller, T.A. Tombrello, Radiat. Eff. 49 (1980) 195.
[35] A. Benninghoven, Angew. Chem. Int. Ed. Engl. 33 (1994) 1023.
[36] K. Mochiji, N. Itabashi, S. Yamamoto, H. Shimizu, S. Ohtani, Y. Kato, H. Tanuma, K. Okuno, N. Kobayashi, Surf. Sci. 357–358 (1996) 673.
[37] K. Mochiji, N. Itabashi, S. Yamamoto, H. Shimizu, S. Ohtani, Y. Kato, H. Tanuma, K. Okuno, N. Kobayashi, Jpn. J. Appl. Phys. 34 (1995) 6861.
[38] F. Aumayr, J. Burgdörfer, G. Hayderer, P. Varga, H.P. Winter, Phys. Scr. T 80 (1999) 240.
[39] F. Aumayr, J. Burgdörfer, P. Varga, H.P. Winter, Comm. At Mol. Phys. 34 (1999) 201.
[40] J.J. Kolodziej, M. Szymonski, Phys. Rev. B 58 (1998) 13204, and references therein.
[41] R.T. Williams, K.S. Song, J. Phys. Chem. Solids 51 (1990) 679.
[42] Y.F. Chen, C.M. Kwei, C.J. Tung, J. Phys. D 25 (1992) 262.
[43] R.A. Baragiola, Nucl. Instr. and Meth. B 78 (1993) 223.
[44] N. Itoh, A.M. Stoneham, Nucl. Instr. and Meth. B 146 (1998) 362.
[45] E.S. Parilis, Nucl. Instr. and Meth. B 116 (1996) 478.
[46] R.L. Fleischer, P.B. Price, R.M. Walker, Nuclear Tracks in Solids, University of California Press, Berkeley, 1975.
[47] R.E. Walkup, Ph. Avouris, Phys. Rev. Lett. 56 (1986) 524.
[48] H.P. Cheng, J.D. Gillaspy, Phys. Rev. B 55 (1997) 2628.
[49] H.P. Cheng, J.D. Gillaspy, Comput. Mater. Sci. 9 (1998) 285.
[50] J. Burgdörfer, Y. Yamazaki, Phys. Rev. A 54 (1996) 4140.
[51] T. Schenkel, Dissertation, Goethe Universität Frankfurt, 1997.
[52] H. Jacobsson, G. Holmén, Phys. Rev. B 49 (1994) 1789.
[53] H. Jacobsson, G. Holmén, J. Appl. Phys. 74 (1993) 6397.
[54] R.C. Hughes, Phys. Rev. B 15 (1977) 2012.
[55] T. Schenkel, A.V. Barnes, A.V. Hamza, D.H. Scheider, Eur. Phys. J. D 1 (1998) 297.
[56] R.E. Johnson, B.U.R. Sundqvist, Phys. Today 45 (1992) 28, and references therein.
[57] P. Stampfli, K.H. Bennemann, Appl. Phys. A 60 (1996) 191.
[58] P. Stampfli, Nucl. Instr. and Meth. B 107 (1996) 138.
[59] J.W. McDonald, D. Schneider, M.W. Clark, D. Dewitt, Phys. Rev. Lett. 68 (1992) 2297.
[60] T. Schenkel et al., Phys. Rev. Lett. 83 (1999) 4273.
[61] L. Huang, J.P. Callan, E.N. Glezer, E. Mazur, Phys. Rev. Lett. 80 (1998) 185.
[62] R.F.W. Herrmann, J. Gerlach, E.E.B. Campbell, Appl. Phys. A 66 (1998) 35.
[63] T. Sekioka, M. Terasawa, T. Mitamura, M.P. Stöckli, U. Lehnert, C.L. Cocke, Nucl. Instr. and Meth. B 146 (1998) 172.
[64] T. Schenkel, K.J. Wu, H. Li, M.W. Newman, A.V. Barnes, J.W. McDonald, A.V. Hamza, J. Vac. Sci. Technol. B 17 (1999) 2331.
[65] E.F. da Silveira, S.B. Duarte, E.A. Schweikert, Surf. Sci. 408 (1998) 28.
[66] H. Li, D.J. Hymes, J. de Larios, I.A. Mowat, P.M. Lindley, Micro, March 1999, p. 35.
[67] A.C. Diebold, P. Lindley, J. Viteralli, J. Kingsley, B.Y.H. Liu, K.-S. Woo, J. Vac. Sci. Technol. A 16 (1998) 1825.